Land Cover Monitoring over Yellow River Basin in China using Remote Sensing

Masayuki MATSUOKA[1], Tadahiro HAYASAKA[1], Yoshihiro FUKUSHIMA[1],
Yoshiaki HONDA[2] and Taikan OKI[3]
[1] Research Institute for Humanity and Nature
[2] Center for Environmental Remote Sensing, Chiba University
[3] Institute of Industrial Science, University of Tokyo
E-mail: matsuoka@chikyu.ac.jp

Abstract

The current status of the study on the land cover monitoring over the Yellow River in China is outlined in this paper. Three kind of optical sensors, MODIS, AVHRR and Landsat have been used in order to understand the recent status and the change for 20 years since 1980 of the land cover. Land cover map is generated from time series of MODIS in 2000. Time series of AVHRR is in production for the change detection. Landsat data will be applied to drastically changed area such as irrigation districts.

1. Introduction

Yellow River in China (figure 1) has been dried up for many days in a year and long distance since 1970s. It is mainly due to the decrease of precipitation in the upstream of the basin and excess water use for the irrigation. Therefore the hydrological model which can deal with the human activity such as dam operation and irrigation has been being developed in Research Revolution 2002 project [1] for the optimal management of river water. Land cover is one of the most important parameter in the model since it reflects human activity as agriculture and it also provides the hydrological characteristics of land surface. The objective of this study is to analyze the land cover and its change for 20 years from 1980 over the Yellow River basin using remote sensing data.

2. Method of the study

The method of this study is shown in figure 2. Three kinds of optical sensor are used depend on its temporal and spatial characteristics. Because the MODIS onboard Terra is new sensor which has been operated since 1999, it is used to understand recent status of the land cover. Land cover classification map has been generated using time series of MODIS product in 2000 combined with DMSP/OLS product. AVHRR has been operated continuously over 20 years and historical data is available since early 80s, hence it is used to detect the change of land cover. The time series of AVHRR data is generated with the spatial resolution of 1 kilometer from the HRPT, LAC and GAC data. Landsat series of sensor i.e. MSS, TM, and ETM+ have quite higher spatial resolution relative to previous two sensors, even though temporal resolution is low in contrast. These data are used for the validation of land cover classification and change detection, and local analysis over the drastically changed area.

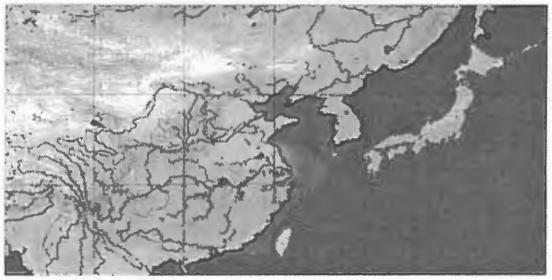

Fig. 1. Yellow River basin.

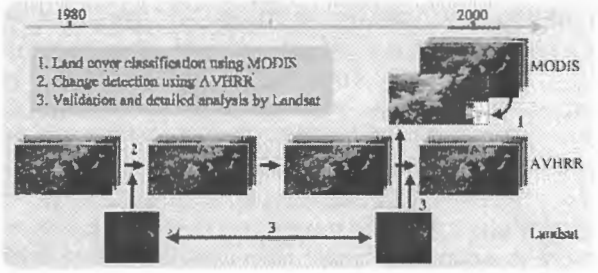

Fig. 2. Method of the study.

3. Land cover classification using MODIS

Land cover map was generated by the classification using time series of MODIS 250 meter resolution reflectance product (MOD09Q1), 500 meter resolution snow product (MOD10A2) and DMSP/OLS nighttime light product in 2000. Eleven kinds of land surface features i.e. annual maximum and minimum NDVI, annual maximum and minimum reflectance in band 1 and 2, annual average reflectance in band 1, monthly average NDVI in April and June, number of snow days in summer season, and human settlements, are derived from MODIS and OLS products (figure 3), and these were input to the simple decision tree classification method shown in figure 4. The threshold values used in decision tree were adjusted manually by comparison of classification result to the other land cover maps. Sixteen types of land cover which include five kinds of agricultural categories were adopted from the hydrological point of view. Classification result is shown in

figure 5. This map was compared to two reference data, existing classification map [2] and Chinese census [3][4]. Land cover map categories were aggregated and compared in province base. The result is shown in figure 6. Forest shows good agreement with land cover map, but overestimation relative to the census. Total agricultural field, grassland and barren show the good agreements in both comparison, but individual agricultural categories i.e. paddy field, dry field, and irrigated field resulted in poor agreements. This classification map is used as the base map in the hydrological model.

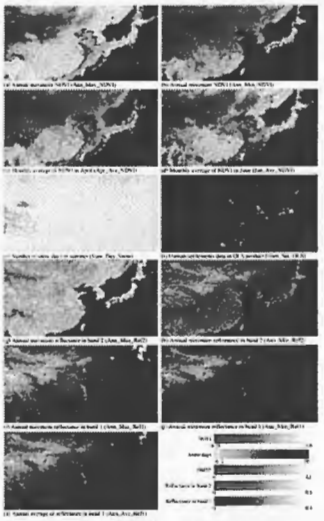

Fig. 3. Land surface features.

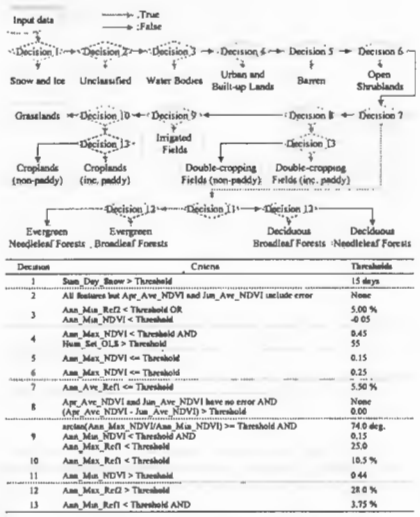

Decision	Criteria	Thresholds
1	Sum_Day_Snow > Threshold	15 days
2	All features but Apr_Ave_NDVI and Jun_Ave_NDVI include error	None
3	Ann_Min_Ref2 < Threshold OR Ann_Min_NDVI < Threshold	5.00 % -0.05
4	Ann_Max_NDVI < Threshold AND Hum_Set_OLS > Threshold	0.45 55
5	Ann_Max_NDVI <= Threshold	0.15
6	Ann_Max_NDVI <= Threshold	0.25
7	Ann_Ave_Ref1 <= Threshold	5.50 %
8	Apr_Ave_NDVI and Jun_Ave_NDVI have no error AND (Apr_Ave_NDVI - Jun_Ave_NDVI) > Threshold	None 0.00
9	arccos(Ann_Max_NDVI/Ann_Min_NDVI) >= Threshold AND Ann_Min_NDVI < Threshold AND Ann_Max_Ref1 < Threshold	74.0 deg. 0.15 25.0
10	Ann_Max_Ref1 < Threshold	10.5 %
11	Ann_Min_NDVI > Threshold	0.44
12	Ann_Max_Ref2 > Threshold	28.0 %
13	Ann_Min_Ref1 < Threshold AND	3.75 %

Fig. 4. Decision tree classification method.

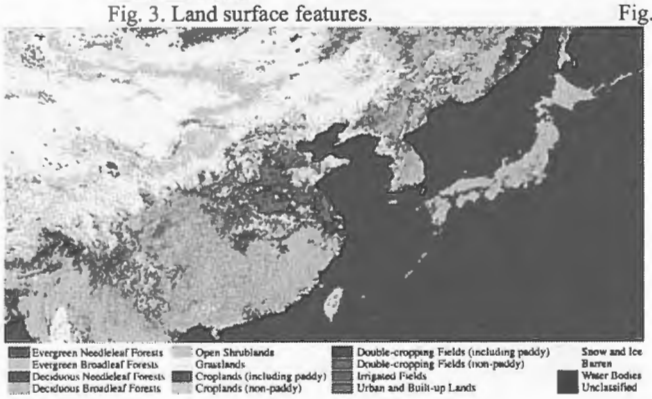

Fig. 5. Classification result.

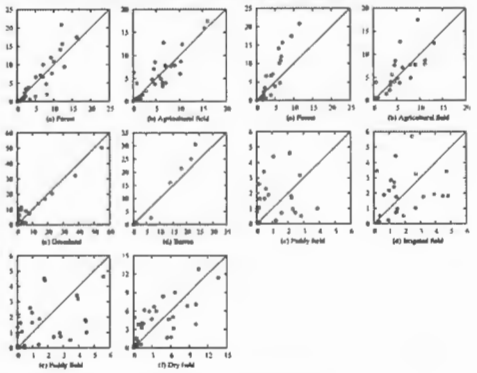

Fig. 6. Comparison to reference data.

4. Change detection using AVHRR

4.1 Production of AVHRR data set

Time series of AVHRR data for 20 years has been being produced from HRPT, LAC and GAC data with 1 km resolution. HRPT was supplied by Kitsuregawa Laboratory [5], University of Tokyo, and LAC and GAC were downloaded from CLASS, NOAA [6]. The radiometric calibration is applied using time varying calibration coefficients to derive the top of atmosphere reflectance for channel 1 and 2. Channel 3 to 5 are converted to blightness temperature by non-linear calibration method[7-10]. In geometric calibration, initial correction is applied by means of Two-Line Element orbital information [11] followed by precise correction based on the ground control points (GCPs) derived from MODIS product. Precise correction is composed of orbital correction and attitude correction. Orbital correction is applied daily several paths at the same time for the purpose to keep the number of available GCPs, and attitude correction is applied by each path in order to allow the frexibility of attitude. Optimized orbital information and attitude angles are derived by least square estimation.

The HRPT data is not available especially in the western region around upstream of the Yellow River, because it is outside of the receivable range of University of Tokyo receiving station. Therefore, GAC is used as base product and HRPT and LAC are overlaid if these are available, though the spatial resolution of GAC is lower as 4 kilometers. The outline of the overlay is shown in figure 7.

4.2 Preliminary study using Pathfinder AVHRR Land Data Set

Change detection method was applied for Quingtongxia and Hetao irrigation districts as the feasibility study

by means of 8 kilometers resolution AVHRR data set, Pathfinder AVHRR Land data set. Annual maximum NDVI (Ann_Max_NDVI) is derived by averaging of second to sixth maximum NDVI among the daily data for one year. Time series of regional distribution of Ann_Max_NDVI for both irrigation districts are shown in figure 8. Ann_Max_NDVI has been increased gradually in both districts through 20 years. The trend is slightly different, that is, widely distributed Ann_Max_NDVI has been concentrated to higher value in Quingtongxia districts, and lower Ann_Max_NDVI has been totally increased in Hetao district. The reason of these increase seems to be the increase of agricultural fields, however, the detail of the change is not interpreted from 8 kilometer resolution data set.

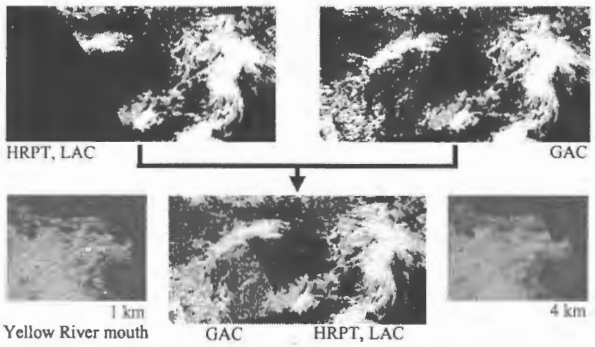

Fig. 7. Overlay of HRPT, LAC (1 km) and GAC (4 km).

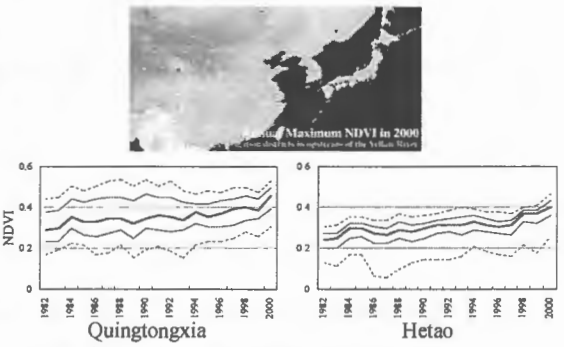

Fig. 8. Time series of the distribution of the annual maximum NDVI for two irrigation districts.

5. Detailed analysis using Landsat

The change of the Ann_Max_NDVI in irrigation districts has been analyzed in detail using higher resolution data, 1 kilometer resolution AVHRR combined with Landsat. The method of analysis is shown in figure 9. Ann_Max_NDVI over Quingtongxia districts in 1999 was derived from 1 kilometer daily AVHRR data described in section 4. Land cover map was derived by simple decision tree classification using Landsat/ETM+ acquired on 12th Aug. 1999 when the status of the vegetation is most active. The data was downloaded from GLCF, University of Maryland [12]. Since the spatial resolution of AVHRR and ETM+ is about 1 kilometer and 28.5 meters respectively, 1 pixel of AVHRR corresponds to 32 by 25 pixels of ETM+. Therefore, fraction of agricultural area (Frac_Agri_Area) in one AVHRR pixel is calculated from the land cover map of ETM+. Finally Frac_Agri_Area is estimated from the Ann_Max_NDVI.

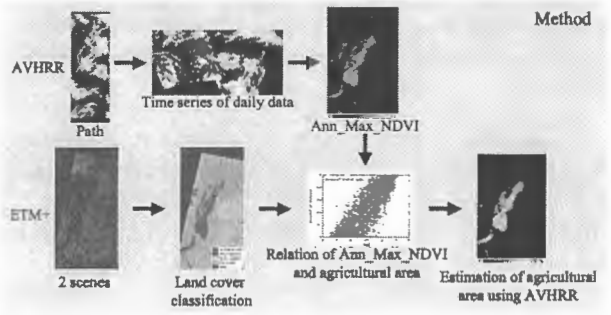

Fig. 9. Method of the analysis.

The decision tree classification method applied to ETM+ is shown in figure 10. NDVI, reflectance in band 5 and digital elevation model GTOPO30 [13] were used to categorize the pixel into the five types of land cover. The classification result is shown in figure 11. As the assessment of the classification accuracy, only agricultural field is compared to county based census value, that is, agricultural area in each county is extracted using county mask (figure 12) and it is compared to the sowing area in 1999 recorded in the Statistical Yearbook of Ningxia province. The result is shown in figure 13. The overestimated counties are located in midstream of the district, and relatively underestimated counties are in downstream. Excess underestimated county is Yanchi county, which is located outside of the irrigation districts.

Ann_Max_NDVI in Quingtongxia district is shown in figure 14. The relation of Ann_Max_NDVI and Frac_Agri_Area is shown in figure 15. The linear equation of [Frac_Agri_Area = 2.54 * Ann_Max_NDVI - 0.33] is derived from the least square regression. The Frac_Agri_Area estimated from AVHRR using this equation is shown in figure 16. The mountainous area was masked by GTOPO30. Figure 17 shows the county based comparison of agricultural area with ETM+ classification. This figure indicates that AVHRR

estimation is comparable to the ETM+ estimation in county base. This method is specialized to irrigation districts in arid region where the contrast of the NDVI in agricultural area and background is high. The method will be applied to the time series of AVHRR for detecting the seamless change of the land cover in irrigation districts.

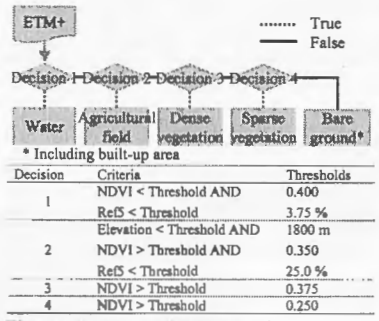

Decision	Criteria	Thresholds
1	NDVI < Threshold AND	0.400
	Ref5 < Threshold	3.75 %
2	Elevation < Threshold AND	1800 m
	NDVI > Threshold AND	0.350
	Ref5 < Threshold	25.0 %
3	NDVI > Threshold	0.375
4	NDVI > Threshold	0.250

Fig. 10 Classification method.

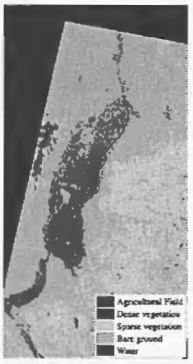

Fig. 11. Land cover map.

Fig. 12. County mask

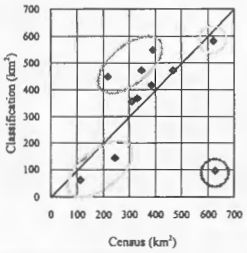

Fig. 13. Comparison result.

Fig. 14. Ann_Max_NDVI

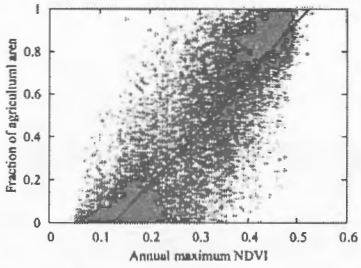

Fig. 15. Relation of Ann_Max_NDVI and Frac_Agri_Area.

Fig. 16. Frac_Agri_Area. derived by AVHRR

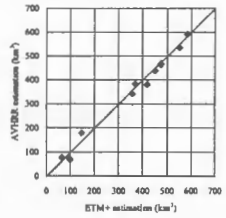

Fig. 17. Comparison

6. Conclusions and future plans

The land cover monitoring on the Yellow River in China is in progress under the hydrological project. Land cover map in 2000 was produced using 250 meter MODIS product and it is used as the base map of the hydrological model. The time series of AVHRR for 20 years has been being produced from HRPT, LAC and GAC with the spatial resolution of 1 km. Land cover change especially concerned with the agricultural field will be detected using this data combined with Landsat.

Acknowledgement

This study has been carried out as a part of the Research Revolution 2002 project supported by the Ministry of Education, Culture, Sports, Science and Technology (MEXT) in Japan.

Authors appreciate the valuable distribution of HRPT by Kitsuregawa Lab., LAC data by Comprehensive Large Array-data Stewardship System, Landsat by Global Land Cover Facility, and GTOPO30 by USGS.

References

[1] The Yellow River Studies. (2003). http://www.chikyu.ac.jp/yris/.
[2] CASW Data Technology, 1 km land-use & land cover raster data of China, http://www.casw.com.cn/.
[3] Chinese Forest Science Data Center website, http://www.cfsdc.org/.
[4] National Bureau of Statistics of China website, http://www.stats.gov.cn/.
[5] Kitsuregawa Laboratory, http://www.tkl.iis.u-tokyo.ac.jp/english/.
[6] NOAA's Comprehensive Large Array-data Stewardship System, http://www.class.noaa.gov/nsaa/products/welcome.
[7] Kidwell, K. B., "NOAA Polar Orbiter Data Users Guide" (November 1998 revision), http://www2.ncdc.noaa.gov/.
[8] Goodrum, G., et al., "NOAA KLM User's Guide" (September 2001), http://www2.ncdc.noaa.gov/.
[9] Agbu, P.A., and M. E. James. (1994). "The NOAA/NASA Pathfinder AVHRR Land Data Set User's Manual", Goddard Distributed Active Archive Center, NASA, Goddard Space Flight Center, Greenbelt.
[10] Ouaidrari, H., et al. (2002). " Land surface temperature estimation from AVHRR thermal infrared measurements An assessment for the AVHRR Land Pathfinder II data set", Remote Sensing of Environment vol. 81, pp. 114-128.
[11] Celes Track, http://www.celestrak.com/.
[12] Global Land Cover Facility, University of Maryland. http://glcf.umiacs.umd.edu/data/.
[13] GTOPO30 Global 30 Arc Second Elevation Data Set http://www1.gsi.go.jp/geowww/globalmap-gsi/gtopo30/gtopo30.html.